International Journal of Secondary Metabolite
2023, Vol. 10, No. 3, 437–458
https://doi.org/10.21448/ijsm.1180610
Published at https://dergipark.org.tr/en/pub/ijsm
Research Article

Antibacterial and antioxidant activity of compounds from *Citrus sinensis* L. peels and *in silico* molecular docking study

Raey Yohannes[1], **Teshome Geremew**[1,*], **Tarekegn Tafese**[1], **Milkyas Endale**[2,*]

[1]Department of Applied Biology, School of Applied Natural Science, Adamma Science and Technology University, P.O. Box 1888, Adama, Ethiopia.
[2]Department of Applied Chemistry, School of Applied Natural Science, Adama Science and Technology University, P.O. Box 1888, Adama, Ethiopia.

Abstract: The increasing prevalence of drug resistance, adverse side effects of existing antibiotics, and the resurgence of previously known infections have necessitated the search for new, safe, and effective antimicrobial agents. The peels of *Citrus sinensis* L. (300 g) were extracted using maceration and ultrasonic-assisted extraction methods with ethanol, resulting in yields of 20.99 g and 11.5 g (7%, 7.5%), respectively. Silica gel column chromatographic separation of the ethanol extract yielded N-(1,3,4,5-tetrahydroxydecan-2-y1) octanamide (**1**), decanoic acid (**2**), β-sitosterol-3-*O*-β-D-glucopyranoside derivative (**3**), and (z)-ethyl tetradec-7-enoate (**4**). GC-MS analysis of the essential oil detected 7 chemical components accounting for 99.84% of the total composition of which limonene was found to be the predominant constituent (87.5%). *In vitro* antibacterial tests revealed promising zones of inhibition by ethanol extract (12.67±0.58 mm, at 150 mg/mL), compound **4** (15.67±2.88 mm, at 6 mg/mL), and compound **1** (12.00±0.00 mm, at 6 mg/mL) against *E. faecalis*, *S. typhimurium*, and *P. aeruginosa*, respectively, compared to gentamicin (13.00±1.73 mm, 18.00±1.00 mm, and 16.67±1.15 mm, respectively at 10 µg/mL). DPPH radical scavenging activity indicated that compound **1** exhibited an IC_{50} value of 0.05 mg/mL, compared to ascorbic acid's 0.016 mg/mL. *In silico* molecular docking studies revealed that compounds **1** and **3** had the lowest scoring poses against *E. coli* DNA gyrase B enzyme, human peroxiredoxin 5, and *S. aureus* pyruvate kinase, respectively. These findings support traditional applications of *Citrus* peels in treating infectious diseases, particularly against Gram-positive strains, and highlight their potential use as antibacterial ingredients in cosmetics.

ARTICLE HISTORY
Received: Sep. 27, 2022
Revised: June. 01, 2023
Accepted: June. 27, 2023

KEYWORDS
Citrus sinesis, Antimicrobial activity, Antioxidant activity, Molecular docking, Essential oils.

1. INTRODUCTION

Infectious diseases are public health problems and a significant cause of death worldwide. Infections due to pathogenic microorganisms cause severe concern for human health. Increasing cases of drug resistance, unwanted side effects of existing antibiotics, and the

*CONTACT: Milkyas Endale, milkyas.endale@astu.edu.et,
Teshome Geremew teshome.geremew@gmail.com Department of Applied Chemistry/Applied Biology, School of Applied Natural Science, Adama Science and TechnologyUniversity, P.O. Box 1888, Adama, Ethiopia.

e-ISSN: 2148-6905 / **© IJSM 2023**

reappearance of earlier known infections have demanded the need for new, safe, and effective antimicrobial agents (Ayukekbong *et al*., 2017; Riffel *et al*., 2002; Shetty *et al*., 2016). Plants have been utilized to treat a variety of diseases and preserve health in various cultures around the world since ancient times (Akinyemi *et al*., 2016). The World Health Organization (WHO) estimates that around 80% of the population still uses herbal remedies to treat various ailments because of their ease of access, low cost, and lack of adverse effects (WHO, 2004). Traditional medicine is used as a primary source of health care by the majority of Ethiopians because it is culturally rooted, accessible, and economical (Koehn & Carter, 2005).

Citrus sinensis L. Osbeck (Sweet orange) commonly called 'orange' is a member of the Rutaceae family and Aurantioideae subfamily. It is a major source of vitamins, especially vitamin C, a sufficient amount of folacin, calcium, potassium, thiamine, niacin, and magnesium (Angew, 2007). Because of its excellent nutritional content, and source of vitamins, it is now produced practically everywhere in the world as a human food source (Etebu & Nwauzoma, 2014). Orange fruits are the primary source of key phytochemical elements and have long been prized for their healthy nutritional and antioxidant characteristics (Tripoli *et al*., 2007). Numerous compounds with antibacterial, antioxidant, and anti-inflammatory properties were isolated from the peels of various *Citrus* fruits (Friedman *et al*., 2002). The present study aims to identify the chemical components of *C. sinensis* peel extracts and essential oils along with an evaluation of their antibacterial, antioxidant activity, and molecular interaction of the isolated compounds with selected protein targets.

2. Materials and Methods

2.1. Sample Collection and Identification

C. sinensis fruits were collected on February 2, 2022, from the Oromia region, Metehara (Merti) farm, Ethiopia. The plant material was identified and voucher specimen number RY-0001was deposited at the National Herbarium of Ethiopia, Addis Ababa University, Ethiopia.

2.2. Extraction

The extraction of *C. sinensis* peel was done by using cold maceration (by ethanol) and ultrasonic-assisted extraction (UAE) methods. For the maceration method, powdered peels (300 g) were soaked in 2.5 L ethanol (99.9%) for 72 h at room temperature with occasional shaking. The extract was filtered using Whatman filter paper number 1 and concentrated using a Rota evaporator at 40 °C. For the ultrasonic-assisted extraction method, powdered peels (150 g) were soaked in 750 mL ethanol (99.9%), placed in to the ultrasonic bath, sonicated for 30 min at a temperature of 45 °C, and filtered with Whatman filter paper number 1. The extract was concentrated using a Rota evaporator at 40 ^{O}C and kept in sterile vials in the refrigerator until further use.

The essential oil was extracted by hydrodistillation in a modified Clevenger apparatus for 2 hr from powdered *C. sinensis* peels (80 g) in 500 mL of distilled water. The condensate (mixture of essential oil and water) was collected in a 100 mL separatory funnel. The essential oil was consecutively separated from the aqueous layer, dried using anhydrous magnesium sulphate, transferred in to a GC-MS vial, and stored at 4 °C. The yield of essential oil of the *C. sinensis* peel was calculated according to the following equation:

$$\text{Yield (\%)} = \frac{\text{Amount of extracted oil (g)}}{\text{Amount of dry plant material}} \text{ x } 100\%$$

2.3. Isolation of Compounds

The crude extract (15 g) obtained was adsorbed on 15 g of silica gel (mesh size 60-120), subjected to silica gel column chromatography (150 g of silica gel), and eluted with increasing

gradient of ethylacetate in *n*-hexane followed by methanol in dichloromethane. A total of 87 fractions each 100 mL were collected. Fractions that showed similar R_f values and the same characteristic color on Thin Layer Chromatography (monitored by UV lamp at 254 nm and 365 nm) were combined. Fraction 40 (eluted with 100% EtOAc) afforded compound **1** (34.4 mg) with a single spot (R_f value of 0.44) on TLC (eluted with 100% EtOAc). Fraction 32 (eluted with 35% EtOAc in *n*-hexane) afforded compound **2** (11.3 mg). Fractions 41-46 (eluted with 100% EtOAc) were combined and purified by silica gel column chromatography gradient mode of ethyl acetate in *n*-hexane and afforded compound **3** (10.1 mg) (eluted with 30% EtOAc in *n*-hexane). Fraction 19 (eluted with 25% EtOAc in *n*-hexane) yielded compound **4** (34.7 mg).

2.4. Phytochemical Screening of Crude Extract

Phytochemical examinations were carried out on ethanol extract of *C. sinensis* peels using standard methods (Sofowora, 1996; Sofowora, 1993; Williams *et al*., 1973).

2.4.1. *Test for steroid*

Two milliliters of acetic anhydride were added to the *C. sinensis* peel crude extract (0.2 g) which was dissolved in 2 mL of sulphuric acid. A color change from violet to blue to green indicates the presence of steroids.

2.4.2. *Test for terpenoid*

The crude extract (0.2 g) was mixed with 2 mL of chloroform. Then 3 mL of concentrated sulphuric acid was added to form a layer (Salkowski test). A reddish-brown coloration at the interface indicated the presence of terpenoids.

2.4.3. *Test for saponins*

C. sinensis peel crude extract (0.2 g) was dissolved in five milliliters of water and the tubes were shaken vigorously, the formation of a 1 cm layer of foam indicates the presence of saponins.

2.4.4. *Test for flavonoids*

The crude extract (0.2 g) was treated with a few drops of sodium hydroxide solution. The formation of intense yellow color, which becomes colorless with the addition of dilute acid, indicates the presence of flavonoids.

2.4.5. *Test for tannins*

The crude extract (0.2 g) was boiled in 20 mL of water in a test tube. The solution was filtered and a few drops of 0.1% Iron III chloride were added. The appearance of a green/bluish-black color indicates the presence of tannins.

2.4.6. *Test for alkaloids*

One milliliter of 1% HCl was added to 3 mL of the peel crude extract. The mixture was heated for 20 min, cooled, and filtered. Then 1 mL of the filtrate was tested with 0.5 mL Mayer's, reagent (Potassium Mercuric Iodide). The formation of a yellow color precipitate indicates the presence of alkaloids.

2.4.7. *Test for phenol*

Ferric chloride test: the peel crude extract (0.2 g) was treated with 3-4 drops of ferric chloride solution. The formation of bluish-black color indicates the presence of phenols.

2.5. GC-MS Analysis of Essential Oil Extract

GC-MS analysis of essential oil was performed by a GC (7890B, Agilent Technologies, USA) coupled with an MS (5977A Network, Agilent Technologies). The GC had an HP-5MS column (30mm × 250 μm internal diameter (i.d.) and 0.25 μm). Helium was used as a carrier gas (flow

rate 1 mL/ min).The initial oven temperature was 100 °C for 2 min and raised from 100 to 280 ºC at the speed of 10 ºC/min (inlet 250 °C; detector 280 °C; splitless injection/purge time 1.0 min), solvent delay 4.00 min. Mass spectra were recorded in electron-impact mode, with ionization energy of mode at 70 eV, scanning the 33-550 m/z range. The volatile compounds in the oil were identified by comparing the mass spectra of the compounds in the oils with those in the database of NIST11 GC-MS libraries.

The retention indices (RIs) for all of the essential oils were determined by co-injection of the sample with a mixture of the homologous series of C_8-C_{25} *n*-alkanes. Identification of components was based on a comparison of their mass spectra (MS) with those of NIST MS search 2.0 and Wiley 275 libraries and with those described by Adams (Hanuš*et al*., 2008).

2.6. Biological Activity

2.6.1. *Antibacterial activity*

In vitro antibacterial activities of *C. sinensis* peel crude extract and isolated compounds were examined. The antibacterial activities were determined against six pathogenic bacterial strains of *Escherichia coli* (ATCC 25922), *Staphylococcus aureus* (ATCC 25923), *Enterococcus faecalis* (ATCC 29212), *Pseudomonas aeruginosa* (ATCC 27853), *Klebsiella pneumonia* (ATCC 700603) and *Salmonella typhimurium* (ATCC 13311) by agar disk diffusion method. The four sets of dilutions (150, 75, 37.5, and 18.75 mg/mL) of *C. sinenses* peel ethanol extract and isolated compounds (6, 3, 1.5, 0.75 mg/mL) were prepared. The strains of bacteria cells were adjusted at 1.5×10^8 colony forming units (CFU/mL). To determine the number of bacteria present, a 0.5 McFarland standard was prepared by combining 0.05 mL of 1 percent $BaCl_2$ and 9.95 mL of 1 percent H_2SO_4 in distilled water. To contrast a bacterial solution, the preparation was stored in a flask. Mueller-Hinton sterile agar plates were inoculated with indicator bacterial strains.

Sterile filter paper disks (Whatman No. 1, diameter = 6 mm) were placed on the inoculated Mueller-Hinton agar plates. From each dilution, 20 µL were taken and dispensed on the filter papers and allowed to stay at 37 °C for 24 h. Control experiments were carried out under similar conditions, by using gentamicin as positive control and DMSO as a negative control. The zones of growth inhibition around the disks were measured after 18 to 24 h. The sensitivities of the bacterial strains to the peel extracts were determined by measuring the sizes of inhibitory zones starting from the edge of the disk to the edge of the clear zone on the agar surface around the disks, and values < 7 mm were considered as not active against microorganisms.

2.6.2. *Determination of minimum inhibitory concentration (MIC)*

Minimum inhibition concentration (MIC) is defined as the lowest concentration of an antimicrobial that will inhibit the visible growth of a microorganism after overnight incubation. The broth dilution method was adopted to find minimum inhibitory concentrations (MICs) of active extracts. *C. sinensis* peel crude extract and isolated compounds that exhibited antibacterial activity in the preceding test were chosen. The initial concentration of the crude (5 mg/mL) and isolated compounds (1.00 mg/mL) were diluted using two-fold serial dilution by transferring 1 mL of crude into 1 mL of sterile nutrient broth and mix it into a vial, and then serially diluted it into 5 vials. Each concentration was inoculated with 0.02 mL of the standardized bacterial cell suspension and incubated for 24 h at 37 °C. The turbidity or cloudiness of the broth was an indicator of bacteria growth in the broth (Galma *et al*., 2021).

2.6.3. *Determination of minimum bactericidal concentrations (MBC)*

Minimum Bactericidal Concentration (MBC) is the lowest concentration of an antibacterial that prevents the growth of an organism after subculture onto media. The broth dilution method was used to determine *C. sinensis* peel crude extract, essential oil, and isolated compounds'

minimum bactericidal concentration. A fresh nutrient broth medium was used to transfer samples from the MIC determination set. A loop full of all the tubes used in the MIC, which did not show bacteria growth inoculated and sub-cultured onto sterile nutrient agar media streak plating by a sterile wire loop. Following that, all agar media were incubated at 37 °C for 24 h after the transfer is completed. The test tubes were examined for growth at the end of the incubation period. The MBC of the crude extract against the particular tested strain was recorded at the lowest concentration that exhibited no microbial growth.

2.6.4. *Antioxidant activity*

DPPH solution (0.1 mM) was prepared in methanol by dissolving 0.04 g DPPH in 100 mL methanol. The solution was kept in darkness for 30 min to complete the reaction. Ethanol extract from the peels was diluted in four test tubes 1000, 500, 250, and 125 µg/mL. From this concentration, 1 mL of each was mixed with 4 mL of 0.04% DPPH. For the compounds, the same procedure was performed. The samples were diluted 100, 50, 25, and 12.5 µg/mL. From each concentration, 1 mL of the concentration was mixed with 4 mL of 0.04% DPPH. The resulting solutions were subjected to a UV-Vis spectrophotometer to record absorbance at 517 nm. The percentage of DPPH inhibition was calculated according to the following formula.

$$\% \text{ of radical scavenging activity} = \frac{Ab_{standared} - Ab_{analyte}}{Ab_{standard}} \times 100$$

$Ab_{standard}$ is absorbance of standard whereas $Ab_{analyte}$ is absorbance of the analyte.

2.7. *In-silico* Molecular Docking Study of Isolated Compounds

2.7.1. *Preparation of protein and ligand*

3D crystal structures of targeted proteins, *E. coli* Gyrase B (PDB ID: 6F86), *S. aureus* Pyruvate Kinase and Human Peroxiredoxin 5 (PDB ID: 1HD2) were chosen as the protein model and retrieved from the Protein Data Bank (http://www.rcsb.org/). The coordinates of the structures were complexed with water molecules and other atoms which are responsible for increased resolution. Crystal structure of *E. coli* Gyrase B 24 kDa with resolution 1.90 Å has one chain co-crystallized with native ligand 4-(4-bromo-1H-pyrazol-1-yl)-6-[(ethylcarbamoyl) amino]-N-(pyridin-3-yl) pyridine-3-carboxamid (C_{17} H_{16} Br N_7 O_2). Crystal structure of *S. aureus* Pyruvate Kinase in complex with a naturally occurring bis-indole alkaloid with resolution: 3.30 Å contains three chains, A, B, C, D, and one native ligand, and four PO_4 groups. (3S, 5R)-3,5-bis(6-bromo-1H-indol-3-yl)piperazin-2-one ($C_{20}H_{16}Br_2N_4O$) found on chain B and D and PO_4 on chain A, B, C, D.

Crystal structure of Human Peroxiredoxin 5, a Novel Type of Mammalian Peroxiredoxin at 1.5 Å Resolution (1HD2) has one chain (A) co-crystalize with benzoic acid ($C_7H_6O_2$) bromide ion (Br^-).Therefore, hetero-atoms (native ligand/ PO_4 groups) to make the active site free for docking and water molecules which may interfere with ligand/receptor binding (Wong & Lightstone, 2011) were removed using discovery studios visualizer and saved in pdb format. Then polar hydrogen atoms and Kollman charges were added for proper optimization (Galma *et al*., 2021) using an MGL tool and saved in PDBQT format.

The structures of test compounds were drawn using chemdraw ultra 8. Energy minimizations of the ligand/compounds were done using chemdraw 3D ultra 8 and stored in .pdb format. Then PDB format of the compounds was treated using MGL, gasteiger charges were added, non-polar hydrogens are merged out and the torsion angle of the ligand was adjusted automatically. Finally, the prepared compound file was saved as PDBQT in the working directory.

2.7.2. *Grid Map preparation and docking*

Compounds **1** and **3** were docked to target proteins *i.e E. coli* DNA gyrase B (PDB ID: 6F86), *S. aureus* Pyruvate Kinase (PDB ID: 3t07), and Human Peroxiredoxin 5 (PDB ID: 1HD2). The active site was identified by studying the interaction between the native ligand and the enzyme. Docking was performed on the active site of the protein. The search was carried out by building a grid box with a volume that is big enough to cover the active site of the protein. Grid box size of 50 ×50× 54 Å points with a grid spacing of 0.375 Å was considered. The docking of proteins was carried out using the Autodock vina program. After the preparation of the configuration file which contains the receptor-name, pdbqt, ligand-name, pdbqt, grid dimension, and exhaustiveness (run repetition) autodock vina run through the command prompt. Docked structure (ligand-protein complex) was prepared using Pymol, and structure analysis was done and visualized using Biovia Discovery Studio 2021.

3. Results and Discussion

3.1. Extract Yield

Peels of *C. sinensis* were extracted using ethanol 99.9% by maceration (300 g) and ultrasonic extraction (150 g) to afford 20.99 g (7%) and 11.5 g (7.5%) yields, respectively, suggesting the ultrasonic extraction (UAE) gave better yield in agreement with previous studies (Saini *et al*., 2019; Safdar *et al*., 2017). In this regard, it can be explained that UAE is based on the principle of acoustic cavitation which is capable of damaging the cell walls of the plant matrix and thereby favoring better yield compared to the maceration technique.

3.2. Phytochemical Screening

Following conventional experimental techniques, phytochemical screening tests were performed to determine the class of secondary metabolites present in the crude extracts. The phytochemical screening tests conducted on ethanol peels extract of *C. sinensis* revealed the presence of alkaloids, flavonoids, tannins, steroids, phenol, and terpenoids whereas saponins were absent (Table 1) suggesting the peels composed of secondary metabolites with significant biological importance.

Table 1. Phytochemical screening results of *C. sinensis* peel crude extract.

Secondary metabolites	Observation
Alkaloid	+
Tannins	+
Flavonoid	+
Steroid	+
Phenol	+
Terpinoid	+
Saponins	-

+ shows presence, -shows absence

3.3. Characterization of Compounds

Silica gel column chromatographic separation of the ethanol extract afforded four compounds **1**-**4** of which compound **3** was isolated herein for the first time from the species.

Compound **1** (Figure 1) was isolated as a greenish solid with an R_f value of 0.44 (eluted with 100% EtOAc). Its ^{1}H NMR spectrum revealed the existence of amide proton at δ 8.02 (s, 1H), and hydroxyl protons at δ 3.9 integrated for two protons. Four methylene protons were observed at δ 2.1 (H-4 to H-7). Terminal methyl groups were observed at δ 0.9 (H-9' and H-8). Its ^{13}C NMR spectrum displayed a carbonyl group (-CO-) at δ 179.3 attributed to amide carbonyl. Carbon signals resonating at δ 65.3 (C-1"), 33.7 (C-2), 31.8 (C-5'), 29.5, 29.4, 29.2, 28.9, 24.8,

and 22.4 belong to methylene groups, supported by DEPT-135 spectrum pointing down, were visible. The presence of three sp^3 oxygenated methine carbons was observed at δ 73.9 (C-3'), 62.9 (C-2'), and 63.1 (C-4'). The terminal methyl groups appeared at δ 10.1 and 13.5. The above spectral data is in good agreement with the ^{13}C NMR spectral data of N-(1,3,4,5-tetrahydroxydecan-2-y1)octanamide (**1**, Figure 1).

Figure 1. Structures of isolated compounds (**1**-**4**).

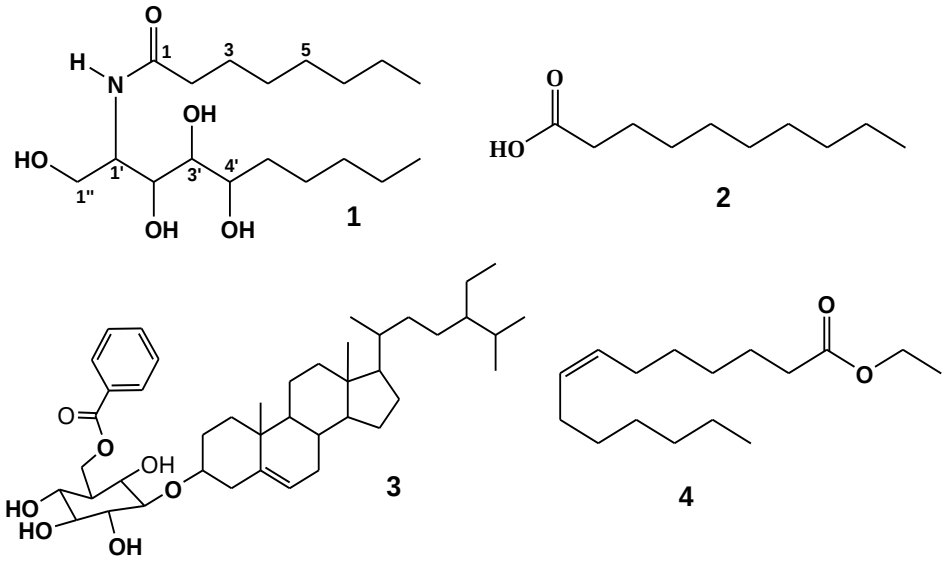

Compound **2** (Figure 1) was obtained as a greenish solid with an R_f value of 0.45 (eluted with 75% EtOAc in *n*-hexane). Its ^{1}H NMR spectral data (Table 2) showed signals that correspond to methylene protons between δ 1.3-1.6 (m, 10H) and signal at δ 2.4 (2H, t). The latter suggests methylene attached to the carbonyl carbon. Terminal methyl protons appeared at δ 0.9 (t, 3H). Its ^{13}C-NMR spectrum showed (Table 2) the carbonyl group (-CO-) of the carboxylic acid at δ 178.7. In addition, peaks at δ 22.7-33.9 correspond to the methylene groups (8 in number) of which the most deshielded one that appeared at δ 33.9 suggests methylene next to carbonyl (C-2). The terminal methyl group appeared at δ 14.1. The above spectral data suggest that the compound is a decanoic acid fatty acid (**2,** Figure 1).

Compound **3** (Figure 1) was isolated as yellowish solid with R_f value of 0.14 (eluted with 30% EtOAc in *n*-hexane). Analysis of the ^{1}H-NMR spectrum ($CDCl_3$, Table 3) demonstrated the presence of six methyl signals at δ 1.0 (s, 1H), 0.9 (d, J = 6.4 Hz, 1H), 0.89 (d, J = 6.5 Hz, 1H), 0.86 (s, 3H), 0.8 (d, J = 1.9 Hz, 1H), and 0.8 (s, 3H). The singlet signal observed at δ 2.4 integrating for two protons suggest the presence of methylene protons adjacent to a carboxyl.

Table 2. ^{1}H NMR and ^{13}C-NMR spectral data of compound **2** ($CDCl_3$, δ in ppm).

Position	Compound **2**		
	^{1}H NMR	^{13}C NMR	Multiplicity
1	-	178.7	Carboxyl
2	2.4 (2H, t),	33.9	CH_2
3	1.6 (2H, m),	24.7	CH_2
4-7	1.3 (8H, m),	29.7, 29.4, 29.2, 29.1	CH_2
8		31.9	CH_2
9		27.7	CH_2
10	0.9 (t, 3H)	14.1	CH_3

Table 3. ^{1}H NMR and ^{13}C NMR spectral data of compound **3** along with literature reported for β-sitosterol 3-*O*-β-D-glucopyranoside.

Position	NMR data of compound **3**		β-sitosterol 3-O-β-D-glucopyranoside (Peshin & Kar, 2017)		
	^{1}H-NMR	^{13}C-NMR	^{1}H NMR	^{13}C NMR	Multiplicity
1	1.0	37.3	1.0 m, 1.40 m	36.8	CH_2
2		29.2	1.58 m, 1.26 m	29.2	CH_2
3	2.4 (d, 2H)	76.1	2.98 m	76.9	CH
4		39.8	1.98 (ddd, 1.98, 12.94, 12.94)	39.3	CH_2
5		140.3		140.4	
6	5.4(t)	122.1	5.35 (t, J = 3.6)	121.2	= CH
7		31.9	1.73 (ddd, J = 2.5, 7.0, 16.0) 1.95 (ddd, J = 16.0, 2.5, 7.0)	31.4	CH_2
8		31.9	1.36 m	31.3	CH
9		50.2	0.85 m	49.6	CH
10		36.7	-	36.2	
11		22.7	1.42 m	20.6	CH_2
12		38.9	1.52 (dd, J = 4.3, 12.37), 1.20 m	38.3	CH_2
13		42.3	-	41.8	
14		56.0	0.95 m	56.1	CH
15		29.7	1.05 m, 1.57 m	28.3	CH_2
16		29.7	1.25 m, 1.85 m	27.8	CH_2
17		55.5	1.20 m	55.4	CH
18	0.70	11.9	0.70 s	11.6	CH_3
19	0.9	19.3	0.94 s	19.1	CH_3
20		34.2	1.40 m	35.5	CH
21		18.8	0.95(d, J = 6.5)	18.6	CH_3
22		37.3	1.20 m	33.3	CH_2
23		29.2	1.25 m	25.4	CH_2
24		45.8	0.94 m	45.1	CH
25		29.2	1.68 m	28.6	CH
26	0.8	19.8	0.87 (d, J = 7.0)	19.7	CH_3
27	0.8	19.0	0.88 (d, J = 7.0)	18.9	CH_3
28		28.2	1.30 m	22.1	CH_2
29	1.0	12.0	0.97 (t, J = 7.5)	11.8	CH_3
1`	3.9	101.2	4.20 (d, J = 7.9)	100.7	CH_2O-
2`		73.6	2.89 (dt, J = 4.5, 8.0)	73.4	CH_3
3’			3.27 (dt, 8.0, J = 4.5, 8.0)	76.9	
4’		70.2	3.00 (dt, J = 4.5, 8.0)	70.0	
5’		76.1	3.06 m(dt, J = 4.5, 8.0)	76.7	
6’	4.0	63.3	4.55 (dd, J = 2.5, 11.77) 4.40 (dd, J = 5.2, 11.77)	62.8	CH_2
1’’		129.3			
2’’ & 6’’		128.2			
3’’ & 5’’		127.8			
4’’		122.0			

The olefinic proton was observed at δ 5.4 (1H, t). Its ^{13}C-NMR (100 MHz, $CDCl_3$, Table 3) spectrum with the aid of DEPT-135 revealed the presence of four quaternary carbon signals observed at δ 174.6, 140.3, 42.3, and 36.7 of which the peaks at δ 174.6 and 140.3 suggest the presence of ester carbonyl and sp^2 quaternary carbons, respectively. Methine signals were observed at δ 56.8, 56.0, 55.5, 50.2, 45.8, 36.1 and 31.9 along with one sp^3 oxygenated methine at δ 70.2 which is a characteristic peak of C-3 methine of steroids. The carbon signals exhibited at δ 39.8, 38.9, 37.3, 34.2, 31.9, 29.7,28.2, 25.00 and 22.7 were due to methylene carbons. The presence of six methyl signals were apparent at δ 19.8, 19.3, 19.0, 18.8, 12.0 and 11.9. The presence of one olefinic methine was observed at δ 122.1. This coupled with the aforementioned sp^2 quaternary carbon at δ 140.3 suggest a characteristics features of sterols with Δ^5 bond. The presence of one glucopyranose moiety is evident from the appearance of one anomeric carbon signal at δ 101.2 along with series of carbon signals at δ 79.6, 76.1, 73.9, 73.6 and 63.3 of which the peak at δ 63.3 suggest oxygenated methylene (C-6') of the glucopyranose moiety. The spectrum revealed a benzoyl moiety peak resonating at δ 174.6, 127.8, 114.5, and 111.0 of which the former suggest ester carbonyl. The above spectral data suggest that the compound is a benzoyl derivative of β-sitosterol-3-*O*-β-D-glucopyranoside (**3**) reported herein for the first time from the species (**3**, Figure 1). This compound was previously reported from flowers of *Viola odorata* L. (Peshin & Kar, 2017).

Compound **4** (Figure 1) was obtained as greenish solid with an R_f value of δ 0.38 (eluted with 25% EtOAc in *n*-hexane). Its ^{1}H-NMR spectrum (400 MHz, $CDCl_3$, Table 4) showed the presence of olefinic proton signals at δ 5.4 (brs, 2H). The presence of oxygenated methylene signal was observed at δ 4.2 (m, 2H). The signal at δ 1.3 (brs,6H) is a characteristic signal for methylene protons which was supported by the appearance of an intense carbon signal at δ 29.7 in the ^{13}C-NMR spectrum. The triplet signal observed at δ 2.3 is ascribed to methylene protons attached to a carboxyl group. The signal at δ 2.0 (s, 2H) belongs to allylic methylene protons.

Table 4. ^{1}H NMR and ^{13}CNMR spectral data of compound **4** ($CDCl_3$, δ in ppm).

Position	NMR data of compound **4**		
	^{1}H-NMR	^{13}C-NMR	Multiplicity
1		179.6	Carboxyl
2	2.3 (t, J = 6.8 Hz, 2H),	34.0	CH_2
3	1.6 (brs, 2H),	24.7	CH_2
4		29.4	CH_2
5		29.7	CH_2
6	2.0 (brs, 2H)	27.2	CH_2
7	5.4 (brs, 1H)	130.0	= CH
8	5.4 (brs, 1H)	129.7	= CH
9	2.0 (brs, 2H)	27.2	CH_2
10		29.4	CH_2
11		29.1	CH_2
12		31.9	CH_2
13		22.7	CH_2
14	0.9 (s, 3H)	14.1	CH_3
1`	4.2 (m, 2H)	65.0	CH_2O-
2`	0.9 (s, 3H)	14.3	CH_3

An up field proton signal at δ 0.9 (s, 6H) is evident for the presence of terminal methyl proton. Its ^{13}C-NMR (100 MHz, $CDCl_3$, Table 4) spectrum with the aid of DEPT-135 revealed a total of 14 carbon signals of which two olefinic methine signals at δ 130.0 and 129.7, and ten methylene signals at δ 34.0, 31.9, 29.7, 29.4, 29.4, 29.3, 29.1, 27.2, 24.7 and 22.7 are clearly evident. Oxygenated methylene was observed at δ 65 (C-1"). The most up field carbon signal

at δ 14.1 accounts for the presence of terminal methyl protons. The existence of ester carbonyl carbon was observed at δ 179.6 (C-1). The above spectral data of the compound is in good agreement with ethyl tetradec-7-enoate (**4**) which was previously isolated from several plants including chloroform extract of stem of *Turraea vogelii* (Hamid *et al*., 2019).

3.4. Essential Oil chemical Composition

The essential oils of *C. sinensis* peel yielded 0.89% (v/w) comparable to literature reports 0.46-2.70% yield from *Citrus* species such as mandarin (2.7%) and orange (0.74%) (Bourgou *et al*., 2012).The GC-MS analysis of essential oils of *C. sinensis* peel revealed that limonene (87.5 %) was the major constituent followed by 1,6-Octadien-3-ol, 3,7-dimethyl (4.35 %), isopulegol (2.46%), pinene (1.93%), trance-p-Mentha-2,8-dienol (1.45%), carveol P294 (1.25%) and 2-cyclohexen-1-one,2-methyl-5-(1-methylethenyl) (0.98%), sequentially (Table 5, Figure 2). The findings of the present work are in a good agreement with previous reports which reported limonene (70-92.5 %) as a major component of *C. sinensis* peels (Mursiti *et al*., 2019). Uraku *et al*.(2020) reported five compounds from GC-MS analysis of methanolic extract of *C. sinesis* peel such as pyridine-2-carbaldehyde, 1-Methyl-1*H*-pyrrole-2-carbaldehyde (40%), glutamic acid (25%), 2-ethyl-5-methyl-1*H*-pyrrole (14%) and pyrrolidin-2-one (12%).

Table 5. Chemical composition of *C. sinensis* peel essential oils analyzed by GC-MS.

No	Name	RT	Molecular Formula	%
1	Limonene	3.74	$C_{10}H_{16}$	87.5
2	2(10)-Pinene	3.261	$C_{10}H_{16}$	1.93
3	1,6-Octadien-3-ol, 3,7-dimethyl-	4.404	$C_{10}H_{18}O$	4.35
4	trans-p-Mentha-2,8-dienol	4.883	$C_{10}H_{16}O$	1.45
5	Isopulegol	5.704	$C_{10}H_{18}O$	2.46
6	Carveol P294	6.05	$C_{10}H_{16}O$	1.25
7	2-Cyclohexen-1-one, 2-methyl-5-(1-methylethenyl)-	6.322	$C_{10}H_{14}O$	0.98

Figure 2. GC-MS Chromatogram of *C. sensis* peel essential oils.

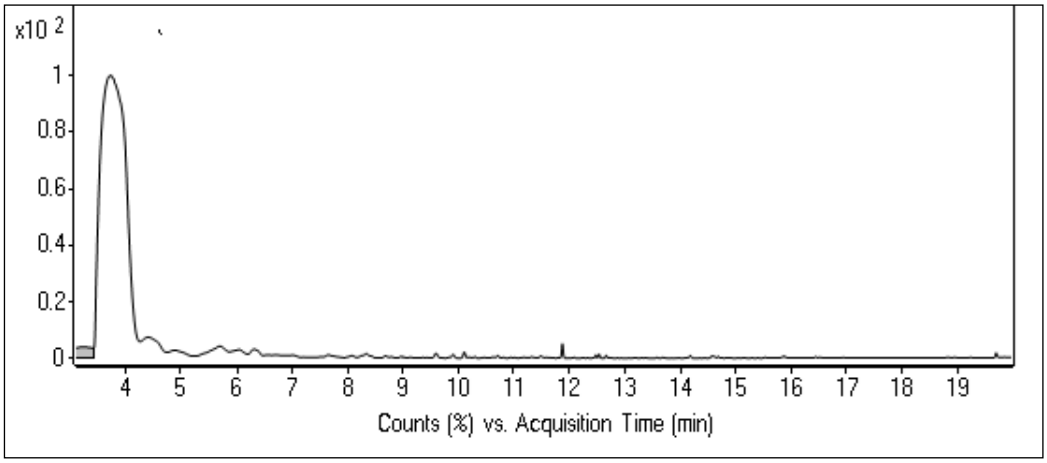

3.5. Antibacterial Activity

3.5.1. *In vitro* antibacterial activity

The ethanol extract of *C. sinensis* peels and isolated compounds were tested for their antibacterial activity in different concentrations against six pathogenic bacterial strains, (*E. coli*, *S. aureus*, *E. faecalis*, *P. aeruginosa*, *K. pneumonia* and *S. typhimurium*) compared to gentamicin as positive control and DMSO as negative control. The mean zone of inhibition

values indicated that all the compounds exhibited a dose-dependent antibacterial activities ranging from 8.00 mm to 15.67 mm. The ethanol extract revealed a promising zone of inhibition against *S. typhimurium* (8.67±1.15 mm), *K. pneumonia* (9.33±0.58 mm) and *E. coli* (9.67±0.58 mm) at 18 mg/mL compared to gentamicin (18.00±1.00 mm, 16.67±2.08 mm and 16.33±1.15 mm, respectively) at concentration of 10 µg/mL. Previous antibacterial activity study of ethanolic extract of *C. sinensis* peel by Nisha *et al*. (2013) revealed 10-16 mm, 11-14 mm, 9-21 mm and 9-18 mm zone of inhibitions against *E.coli*, *K. pneumonia*, *P. aeruginosa*, and *S. typhi* compared to standard antibiotics which is in good agreement with the findings of our study (Table 6).

β-sitosterol 3-*O*-β-D-glucopyranoside derivative (**3**) (6 mg/mL) showed good activity against *K. pneumonia* (11.00±0.00mm) at 0.75 mg/mL compared to gentamicin (16.67±2.08 mm) at 10 µg/mL. Compound **4** (6 mg/mL) showed a good antibacterial activity against *S. typhimurium* (15.33±2.89 mm), and *E. coli* (10.67±0.58 mm) at 0.75 mg/mL compared to gentamicin (18.00±1.00 mm, 16.33±1.15 mm and 16.67±1.15 mm, respectively) at 10 µg/mL. Compound **1** showed a good zone of inhibition against *K. pneumonia* (10.67±0.58 mm) at 0.75 mg/mL compared to gentamicin (16.67±2.08mm) at 10 µg/mL. Compound **2** (6 mg/mL) exhibited promising zone of inhibition against *P. aeruginosa* (11.67±0.58 mm) and *K. pneumonia* (11.00±0.00 mm) at 6 mg/mL compared to gentamicin (16.67±1.15 mm and 16.67±2.08 mm, respectively) at 10 µg/mL (Table 6).

Table 6. Antibacterial activity of *C. sinensis* peel crude extract.

Sample	Conc (mg/mL)	Inhibition Diameter (mm)±SD					
		E. coli	*S. aureus*	*K. pneumonia*	*S. typhimurium*	*E. faecalis*	*P. aeruginosa*
Ethanol extract	150	10.33±0.58	9.00±1.00	11.33±0.58	10.00±0.00	12.67±0.58	8.67±1.15
	75	10.33±0.58	7.67±0.58	10.67±0.58	8.67±1.52	11.00±0.00	8.33±0.58
	37	10.00±1.00	7.33±0.58	9.67±1.15	7.67±0.58	8.33±1.52	8.00±1.00
	18	9.67±0.58	7.00±0.00	9.33±0.58	8.67±1.15	6.33±0.58	7.00±0.00
Compound **1**	6	10.67±0.58	9.67±1.53	10.00±0.00	9.67±1.15	10.00±0.00	12.00±0.00
	3	10.00±0.00	9.00±0.00	9.67±0.58	9.00±0.00	10.00±0.00	11.33±0.58
	45047	10.67±0.58	8.00±1.00	10.33±0.58	9.33±0.58	10.00±0.00	11.00±00
	0.75	10.00±1.00	8.00±1.00	10.67±0.58	9.67±0.58	10.00±0.00	10.00±1.00
Compound **2**	6	9.00±1.00	9.33±1.15	11.00±0.00	10.67±0.58	NA	11.67±0.58
	3	9.00±1.00	9.00±0.00	10.00±0.00	9.67±0.58	NA	9.67±0.58
	45047	8.33±1.53	8.00±1.00	9.00±0.00	8.67±0.58	NA	9.33±0.58
	0.75	8.33±1.15	8.00±1.00	9.00±0.00	8.00±0.00	NA	9.00±0.58
Compound **3**	6	10.33±0.58	NA	10.00±0.00	12.00±1.00	NA	NA
	3	9.00±1.00	NA	10.00±0.00	9.00±1.00	NA	NA
	45047	9.33±0.58	NA	10.00±0.00	9.33±0.58	NA	NA
	0.75	8.33±1.15	NA	11.00±0.00	8.33±1.15	NA	NA
Compound **4**	6	11.33±0.58	9.00±2.00	11.33±0.58	15.33±2.89	NA	11.00±1.00
	3	11.00±1.00	8.33±2.08	11.00±0.00	15.67±1.15	NA	9.00±1.00
	45047	11.00±0.00	8.33±1.52	9.67±1.15	13.00±1.73	NA	8.33±0.58
	0.75	10.67±0.58	8.00±1.15	10.67±0.58	15.67±2.08	NA	8.67±0.58
Gentamycin	10µg/mL	16.33±1.15	18.67±0.58	16.67±2.08	18.00±1.00	13.00±1.73	16.67±1.15

The antibacterial activity of plants is believed to be due to secondary metabolites such as; tannins, terpinoid, phenol, steroid, alkaloid and flavonoids. Tannin observed in *C. sinensis* peel extract has been found to form irreversible complexes with proline rich protein resulting in the inhibition of cell protein synthesis (Shimada, 2006). Flavonoids have antibacterial and antioxidant characteristics (Hodek *et al*., 2002). Terpenoids present in ethanolic extract of *C. sinensis* are thought to play a role in membrane disruption caused by lipophilic substances (Almas *et al*., 2005). The presence of various secondary metabolites in the *C. sinensis* peel could explain for their function as antibacterial agents. The antibacterial activity evaluation of

the present study showed promising antibacterial activity by ethanol extracts of the peels of *C. sinensis* against *K. pneumonia* and *E. faecalis*, compound **1** against *K. pneumonia*, compound **2** against *P. aeruginosa* and *K. pneumoni*, and compound **4** against *S. typhimurium*, *E. coli* and *P. aeruginosa* and this finding agrees with previous studies by Baba *et al*. (2018). Previous studies by Osarumwense (2017) revealed that the methanolic extract of *C. sinensis* peel is highly active against Gram positive, Gram negative bacteria and fungi at concentrations of 100 mg/mL, 150 mg/mL and 200mg/mL, respectively. Similarly, a related study by Omodamiro and Jamoh (2014) suggested that ethanolic extracts at different concentrations (250, 125, 62.5, 31.25, and 15.5 mg/mL) exhibited antibacterial activity against *S. aureus, S. pneumoniae, E. coli, P. mirabilis* and *P. aeruginosa*, in a dose-dependent manner. Thus, the findings of our study are in a good agreement with the previous studies done of the antibacterial activity of various extracts of the peels of *C. sinensis*.

The essential oils showed promising activity against *S. aureus* (10.67±0.58 mm), *E. coli* (10.67±0.58 mm), *S. typhimurium* (10.67±0.58 mm), *K. pneumonia* (10.33±0.58 mm), *E. faecalis* (10.67±1.15 mm) and *P. aeruginosa* (9.67±1.52 mm) compared to gentamicin (18.67±0.58 mm, 16.33±1.15 mm, 18.00±1.00 mm, 16.67±2.08 mm, 13.00±1.73 and 16.67±1.15, respectively) at concentration of 10 µg/mL (Table 7). Previous studies by Edogbanya *et al*. (2019) revealed higher antibacterial activity of the essential oils against *S. aureus* among the tested bacterial strains which is in a good agreement with the present study. This finding is supported by the results of Burt *et al*. (2004) which showed that Gram-positive bacteria are generally more sensitive to *Citrus* essential oil than Gram-negative. In a related study by Chee *et al*. (2009) and Young *et al*. (2013) limonene is reported to have antibacterial and antifungal properties. Limonene now is known as a significant chemopreventive agent with potential value as a dietary anti-cancer agent in humans (Crowell *et al*., 1994).

Table 7. Antibacterial activity of *C. sinensis* essential oils.

	Conc (mg/mL)	Inhibition Diameter (mm)±SD					
		E. coli	*S. aureus*	*K. pneumonia*	*S. typhimurium*	*E. faecalis*	*P. aeruginosa*
Essential oil	95	12.33±0.58	14.33±1.52	12.00±1.00	12.00±0.00	12.67±0.58	10.67±0.58
	47	12.00±0.00	12.67±0.58	11.67±0.58	11.33±1.15	11.33±0.58	10.67±0.58
	23	11.33±0.58	11.33±0.58	11.33±0.58	11.00±1.00	11.67±0.58	10.33±1.15
	11	10.67±0.58	10.67±0.58	10.33±0.58	10.67±0.58	10.67±1.15	9.67±1.52
Gentamycin 10 µg/mL		16.33±1.15	18.67±0.58	16.67±2.08	18.00±1.00	13.00±1.73	16.67±1.15

3.5.2. *Minimum inhibitory concentration* (MIC)

In the present study, the MIC value obtained from *C. sinensis* peel crude extract, and isolated compounds showed a difference in the inhibitory concentrations against test bacteria (Table 8). The MIC value of the crude extract has been found to be 1.25 mg/mL against *E. coli*, *K. pneumoniae* and *P. aeruginosa* and 2.5 mg/mL against *S. aureus* which is in good agreement with the previous study that revealed MIC value of 1.25 and 2.5 mg/mL against *E. coli* and *P. aeruginosa*, respectively, (Baba *et al*., 2018). Compound **3** showed MIC value (0.25 mg/mL) against *S. typhimurium* and *E. coli*, respectively. Compounds **1** and **2** had the same MIC values at 0.25 mg/mL and 0.5 mg/mL against *P. aeruginosa* and *S. aureus*, respectively. Compound **4** showed MIC value of 1 mg/mL against *P. aeruginosa.*

3.5.3. *Minimum Bactericidal Concentration* (MBC)

MBC values of *C. sinensis* peel crude extract (Table 8) were the same for *P. aeruginosa, E.coli* and *K. pneumoniae* with 2.5 mg/mL value and 5 mg/mL for *S. aureus* which is a better finding compared to that of Baba *et al*. (2018), which reported MBC value of 10 mg/mL, 5 mg/mL

against *S. aureus* and *E.coli*, respectively, and no antibactericidal activity against *P. aeruginosa*. MBC value of the essential oil was similar against *P. aeruginosa* and *S. aureus* with 5 mg/mL value. Compounds **1-3** displayed similar MBC value (0.5 mg/mL) against *P. aeruginosa* and *E. coli.* Compound **1** and **3** showed MBC value (1.00 mg/mL) against *S. typhimurium* and *S. aureus.* Compound **4** showed MBC value (2.00 mg/mL) against *P. aeruginosa* and *S. aureus*.

Table 8. Comparison between MIC and MBC antibacterial values of ethanol extract and compounds.

Bacterial strains	MIC and MBC mg/mL									
	Ethanol extract		Compound **1**		Compound **2**		Compound **3**		Compound **4**	
	MIC	MBC	MIC	MBC	MIC	MBC	MIC	MBC	MIC	MBC
E. coli	1.25	2.5					0.25	0.5		
S. aureus	2.5	5	0.5	1	0.5	1			1	2
K. pnumonia	1.25	2.5								
S. typhimurium							0.5	1		
P. arognosa	1.25	2.5	0.25	0.5	0.25	0.5			1	2
E. fecalis	1.25	2.5								

3.6. Antioxidant Activity

Antioxidant activity of the crude extract, and isolated compounds were measured based on their free radical scavenging activity, determined by the 1,1-diphenyl-2-picryl-hydrazyl (DPPH) method. By this method, it is possible to determine the radical scavenging power of an antioxidant by measuring the decrease in the absorbance of DPPH at 517 nm. As a result of the color changing from purple to yellow, the absorbance was decreased when the DPPH radical is scavenged by an antioxidant through donation of hydrogen to form a stable DPPH-H molecule (Nishibe *et al*., 1995).Lower absorbance of the reaction mixture indicated higher free radical scavenging activity.

Ethanol extract, and isolated compounds of *C. sinensis* peels were tested for their free radical scavenging activities in the DPPH scavenging assay by reacting with stable DPPH radicals. The DPPH radical scavenging activities (%) of ethanol extract, and isolated compounds were found to be 55.69% (compound **1**), 36.15% (compound **2**) 20.7% (compound **3**), 23.8% (compound **4**), 39.94% (crude) at 100 and 1000 µg/mL for the compounds and crude, respectively.

It was observed that the DPPH scavenging activity showed increment in a dose-dependent manner of which compound **1** exhibited the highest percent inhibition of the DPPH compared to ethanol extract and isolated compounds. Ascorbic acid, positive control (µg/mL), showed maximum scavenging effect at very low and high concentration 78, 83, 91% at 25, 50 and 100 µg/mL. Antioxidants have the capability to slow down or prevent the oxidation process of other molecules. In general when compared to standard ascorbic acid, the DPPH radical scavenging activity of ethanol extract of *C. sinensis* peels was found to be lower (Table 9), nevertheless, the activity displayed by the extract increased in a dose dependent which is in a good agreement with previous studies (Akinyemi *et al*., 2016). Based on data in Table 9, the lowest IC_{50} value was displayed by ascorbic acid (0.016 mg/mL), followed by compound **1** (0.5 mg/mL), compound **2** (0.212 mg/mL), compound **3** (50 mg/mL) and compound **4** (2000 mg/mL).

Table 9. DPPH radical scavenging activities (%) of the isolated compounds.

Conc (µg/mL)	Control	Compounds									
		Compound **4**		Compound **3**		Compound **2**		Compound **1**		Ascorbic Acid	
		A	%RSA	A	%RSA	A	%RSA	A	%RSA	A	%RSA
100	1.029	0.784	23.81	0.657	36.15	0.816	20.7	0.702	55.69	0.085	91.74
50	1.029	0.804	21.87	0.736	28.474	0.834	18.95	0.631	49.95	0.168	83.67
25	1.029	0.831	19.24	0.744	27.7	0.839	18.46	0.572	31.2	0.22	78.62
12.5	1.029	0.873	15.16	0.778	24.39	0.883	14.19	0.667	25.56	0.67	34.89
IC_{50} (mg/mL)		50		0.212		2000		0.05		0.016	

Conc (µg/mL)	Control	Ethanol extract		Ascorbic acid	
		A	%RSA		
1000	1.029	0.618	39.94	0.04	96.11
500	1.029	0.71	31	0.045	95.63
250	1.029	0.745	27.6	0.047	95.43
125	1.029	0.825	19.83	0.05	95.14
IC_{50} (mg/mL)		3251.785			

Conc-Concentration, A- Absorbance, %RSA- Radical Scavenging Activity (%)

3.7. *In silico* Molecular Docking

Two compounds were docked in this study against three organism targets proteins in order to predict their orientation and binding affinity at the active site of the receptor. For each compound nine poses were generated with different binding energy and RMSD value. But the dock pose with least binding energy and RMSD value has the highest affinity are considered as the best docked conformation (Azam & Abbasi, 2013).

3.7.1. *Docking of against E. coli DNA gyrasee B enzyme*

Compounds **1** and **3** were docked against *E. coli* DNA gyrase B (PDB ID: 6F86) enzyme and displayed binding affinity of -6.2 Kcal/mol and -6.9 Kcal/mol, respectively, compared to gentamicin (-7.3 Kcal/mol) (Figure 3a, b, Table 10).

Table 10. Compound **1**, **3** and gentamicin binding energy with *E. coli* DNA gyrase B**(**PDB ID: 6F86).

Ligands	Affinity (kcal/mol)	H-bond	Residual amino acid interactions	
			Hydrophobic/Pi-Cation	Van der Waals
1	-6.2	GLU-50	ALA-47, A: VAL-43, A: ILE-78and A: ILE-94	VAL-71, A: VAL-167, A: THR-165, A: ASP-73, A: ASN-46, A: PRO-79, A: ASP-49, and A: ARG-76, GLY-76
3	-6.9	ASP-73, GLY-77	ARG-76 and A: ALA-53, and A: ILE-94	VAL-93, VAL-120, VAL-97, LEU-98, SER-121, VAL-188, GLY-119, GLY-117, PRO-79 and ASN-46, ALA-47, THR-165, GLU-50, ASP-49, ILE-78
Gentamicin	-7.3	GLY-77, GLU-30, THR-165, ASP-73, ARG-46	PRO-79, ILE-94	ASP-49, ALA-47, ILE-78, GLY-164, GLY-73, ARG-76

Figure 3a. Interaction of compound **1** on *E. coli* DNA gyrase B (PDB ID: 6F86) ((A) 2D interaction, (B) 3D interaction).

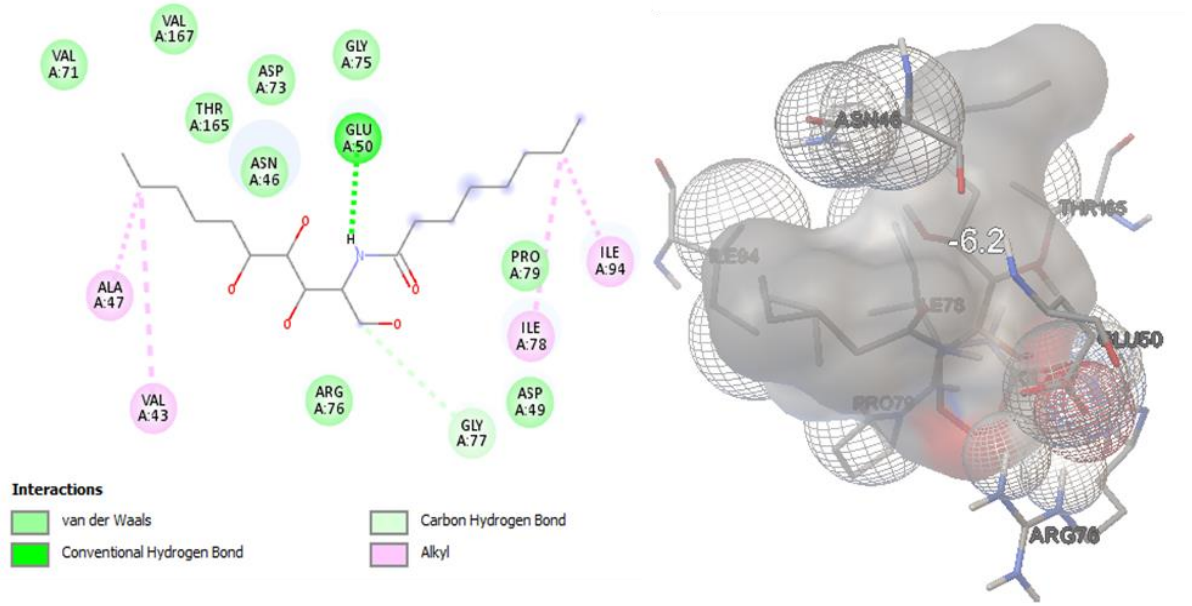

Figure 3b. Interaction of compound **3** on *E. coli* DNA gyrase B (PDB ID: 6F86) (A) 2D interactions (B) 3D interactions.

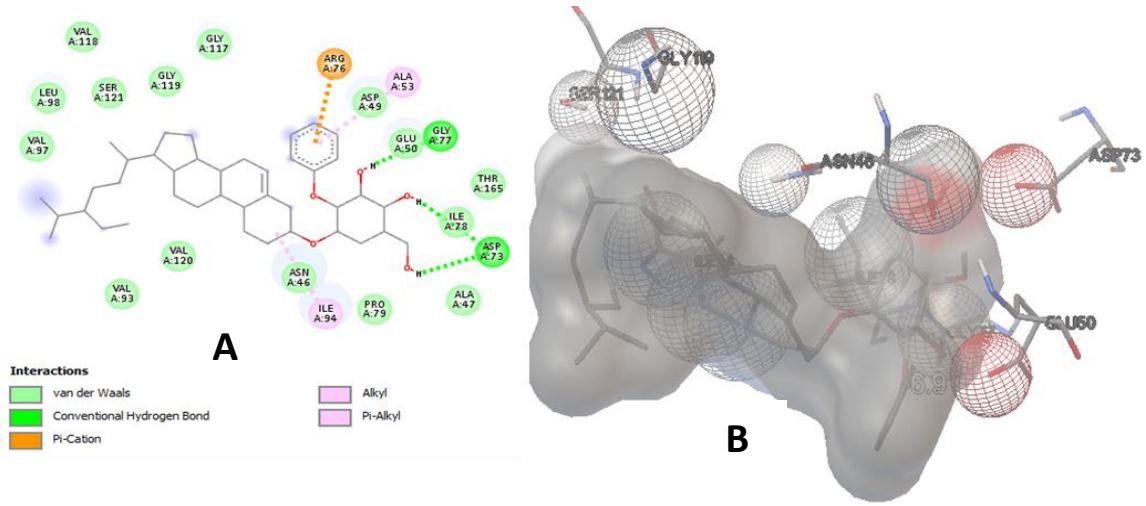

3.7.2. *Docking against human peroxiredoxin* 5

Compounds **1** and **3** were docked against Human Peroxiredoxin 5(PDB ID: 1HD2) enzyme and displayed binding affinity of -5 Kcal/mol and -7.1 Kcal/mol, respectively, compared to ascorbic acid (-5.6 Kcal/mol) (Figure 4a, b; Table 11).

Figure 4a. Interaction of compound **1** against Human Peroxiredoxin 5 (PDB ID: 1HD2) (A) 2D interactions (B) 3D interactions.

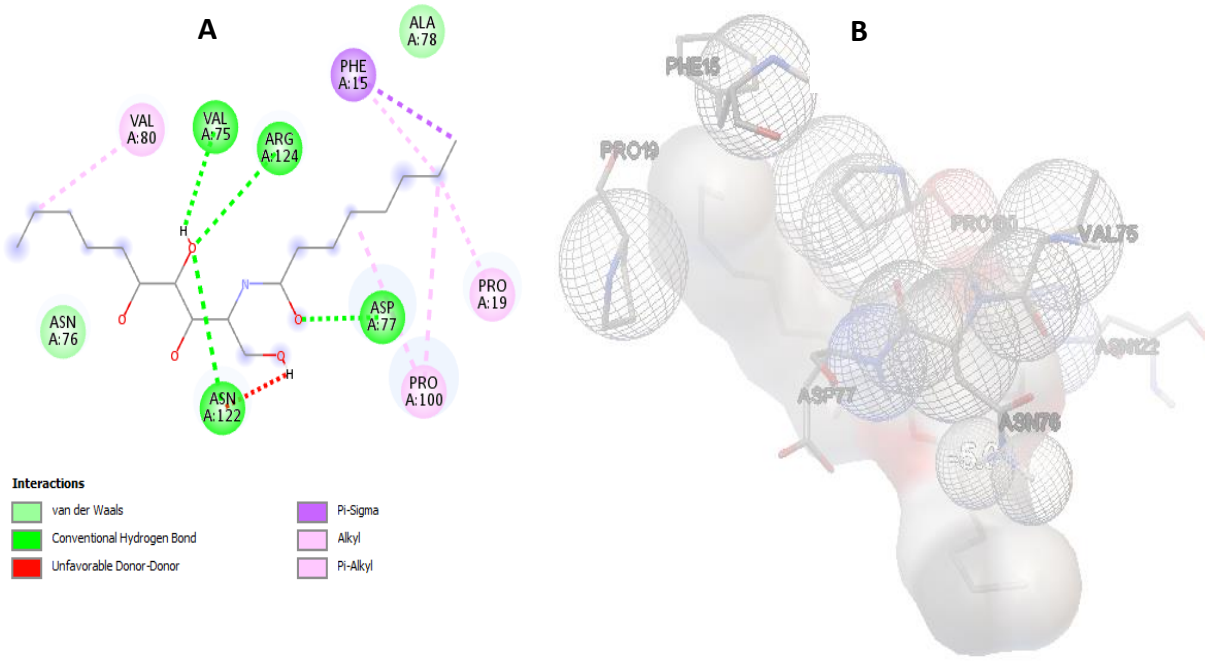

Figure 4b. Interaction of compound **3** against Human Peroxiredoxin 5 (PDB ID: 1HD2) (A) 2D interactions (B) 3D interactions.

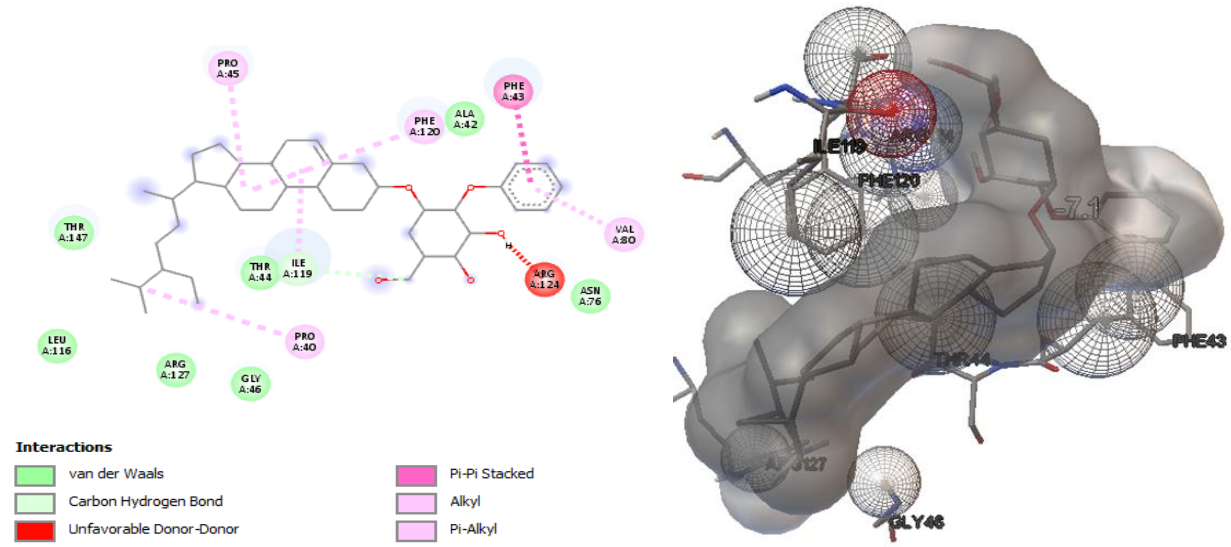

Table 11. Different binding energy and RMSD value of compound **1**, **3** and ascorbic acid against Human Peroxiredoxin 5 (PDB ID: 1HD2).

Ligands	Affinity (kcal/mol)	H-bond	Residual amino acid interactions	
			Hydrophobic/Pi-Cation	Van der Waals
1	-5	VAL-75, ARG-124, ASN-122, ASP-77	PHE-15, VAL-80, PRO-19, PRO-100	ASN-76, ASN-78, GLU-50
3	-7.1		ARG-124, VAL-80, PRO-40, PRO-45, PHE-120, PHE-43	THR-147, LEU-116, ARG-127, GLY-46, THR-44, ASN-76, ALA-42
Ascorbic acid	-5.6	ARG-86 GLY-82 GLU-91	-	GLU-16, LYS-93, GLY-92, VAL-94, ARG-95, ALA-90, GLY-17, GLY-85

3.7.3. *Docking against of S. Aureus pyruvate kinase*

Compounds **1** and **3** were docked against *S. aureus* Pyruvate Kinase (PDB ID: 3t07) enzyme and displayed binding affinity of -6.6 Kcal/mol and -8.2kcal/mol, respectively, compared to gentamicin (-7.7 Kcal/mol) (Figure 5a, b; Table 12).

Table 12. Different binding energy and RMSD value of compound **1**, **3** and gentamicin against *S. aureus* Pyruvate Kinase (PDB ID: 3t07) protein target.

Ligands	Affinity (kcal/mol)	H-bond	Residual amino acid interactions	
			Hydrophobic/Pi-Cation	Van der Waals
1	-6.6	GLN-574, LEU-471, ILE-469, THR-463, HIS-470, ASN-465, LYS-468, GLU460	PHE-578, LEU -471	GLY-462, THR-461, PRO-457, VAL-456, LEU-355, ASP-571, ALA-582, ASN-583, LEU-449, GLU-475, LYS-576, ASP-474, GLY-473
3	-8.2	LEU-269	LYS-390, ALA-573, Val-356	THR-461, GLY-462, THR-463, SER-383, ASP-237, LYS-271, ARG-386, ASN-357, GLY-270, ARG-484, GLY-575, GLY 481, GLY 479, GLN-480, LYS-576, GLN-574, ALA-572
Gentamicin	-7.7	LYS-271, ASP-237, GLU-234, ARG-386, THR-387	ALA-374, VAL-336	GLN-374, VAL-233, GLY-483, ILE-482, LEU-343, ASN-337, SER-383, THR-463, SER-236

Figure 5a. Interaction of compound **1** against *S. aureus* Pyruvate Kinase (PDB ID: 3t07) protein target(A) 2D interactions (B) 3D interactions.

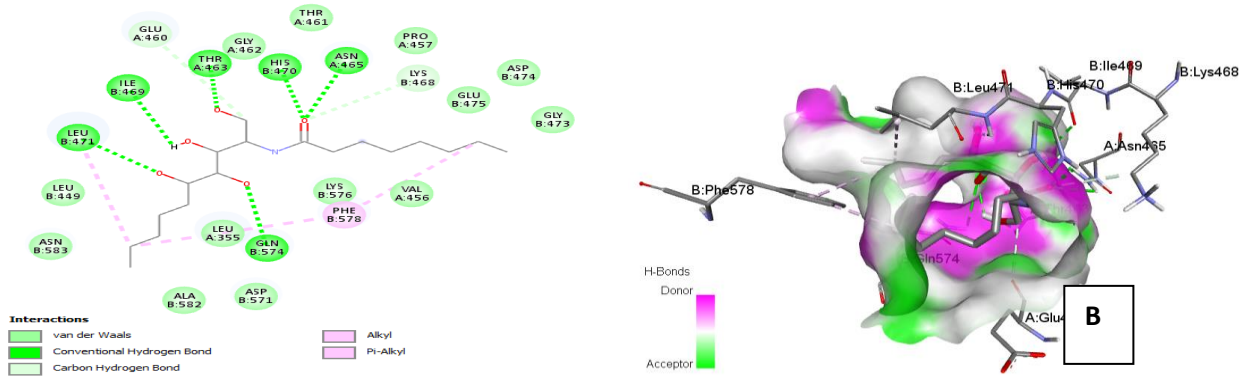

Figure 5b. Interaction of compound **3** against *S. aureus* Pyruvate Kinase (PDB ID: 3t07) protein target(A) 2D interactions (B) 3D interactions.

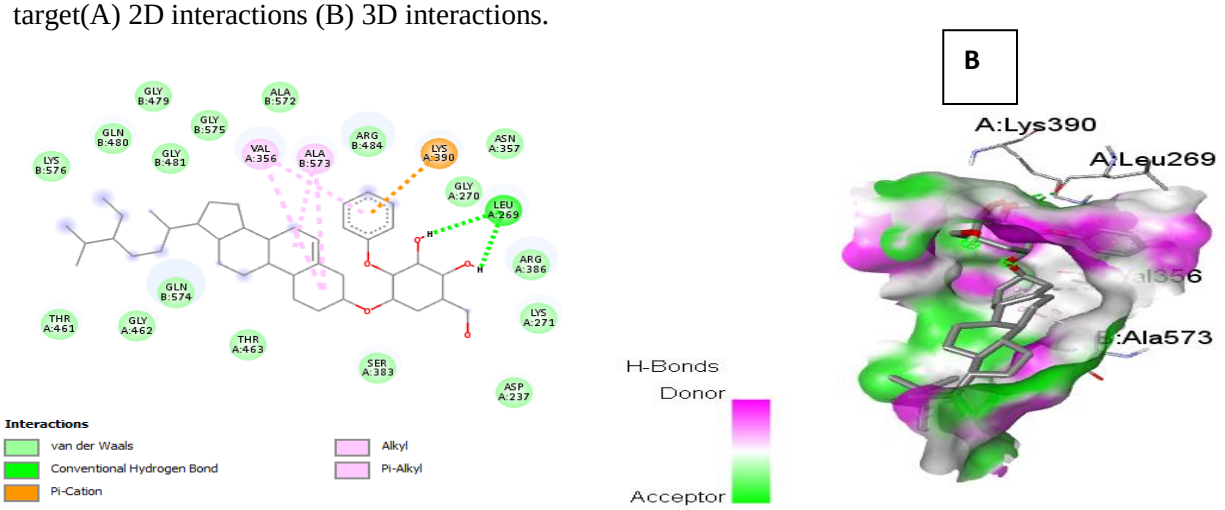

5. CONCLUSION

The presented study identified *N*-(1,3,4,5-tetrahydroxydecan-2-y1) octanamide (**1**), decanoic acid (**2**), β-sitosterol 3-*O*-β-D-glucopyranosidederivative (**3**) and (z)-ethyl tetradec-7-enoate (**4**) compounds from ethanol peels extracts of *C. sinensis* of which compound **3** was identified herein for the first time from the species. The essential oils from peels of *C. sinensis* peel were analyzed by GC-MS which revealed the presence of seven chemical components accounting for 99.84 % of the total compositions of which limonene (87.5%) was the major constituent followed by 1,6-Octadien-3-ol,3,7-dimethyl- (4.3%), isopulegol (2.46%), pinene (1.9%), and trance-p-Mentha-2,8-dienol (1.45%), respectively. The therapeutic effects of limonene have been extensively studied, proving antioxidant, anticancer, antifungal, antiviral, and gastroprotective effects, among other beneficial effects in health. Thus, the high composition of limonene in essential oils from peels of *C. sinensis* suggest the potential of the oils as food additives and cosmetic ingredients.

The ethanol extract revealed a promising zone of inhibition against *S. typhimurium* (8.67±1.15 mm), *K. pneumonia* (9.33±0.58 mm) and *E. coli* (9.67±0.58 mm) at 18 mg/mL compared to gentamicin (13.00±1.73 mm, 18.00±1.00 mm, 16.67±2.08 mm and 16.33±1.15 mm, respectively) at concentration of 10 µg/mL in agreement with previous study by Najimu (2013). Compound **1** also displayed promising antibacterial activity against K. *pneumonia,* compound **2** against *P. aeruginosa* and *K. pneumoni* and compound **4** against *S. typhimurium* and *E. coli*. The high antibacterial activity of the ethanol extract may be attributed to the synergistic effects of these constituents present in the extract. The essential oil of *C. sinensis* peels had promising antibacterial activity against *S. aureus* (10.67±0.58 mm) and *E. faecalis* (10.67±1.15 mm) at 11 mg/mL compared to gentamicin (18.67±0.58 mm and 13.00±1.73 mm, respectively) at concentration of 10 µg/mL. DPPH radical scavenging activity revealed that compound **1** showed IC_{50} value of 0.05 mg/mL compared to ascorbic acid 0.016 mg/mL indicating the potential of the plant as natural antioxidant remedies.

Compounds **1** and **3** were docked against *E. coli* DNA gyrasee B, Human Peroxiredoxin 5 and *S. aureus* Pyruvate Kinase enzymes and displayed binding affinity of -6.2/-6.9 Kcal/mol, -5/-7.1 Kcal/mol, and -6.6/-8.2 Kcal/mol, respectively, compared to gentamicin (-7.3 Kcal/mol), and ascorbic acid (-5.6 Kcal/mol), respectively. Therefore, the *in vitro* antibacterial, DPPH radical scavenging activity along with the molecular docking analysis suggest the potential use of the peels of *C. sinensis* as promising antibacterial agents which corroborates the traditional uses of the peels of the plant. Moreover, the findings of this study suggest the potential of essential oils as antibacterial ingredients in cosmetic applications.

Acknowledgments

The authors are thankful to Adama Science and Technology University (ASTU) for providing MSc study opportunity to RY.

Declaration of Conflicting Interests and Ethics

The authors declare no conflict of interest. This research study complies with research and publishing ethics. The scientific and legal responsibility for manuscripts published in IJSM belongs to the author(s).

Authorship Contribution Statement

Raey Yohannes: Conducted experimental work and wrote the original draft. **Milkyas Endale (PhD)** and **Teshome Geremew (PhD):** Supervised the experimental work and edited the manuscript. **Tarekegn Tafese:** conducted computationally analysis.

Orcid

Raey Yohannes https://orcid.org/0000-0002-1080-5174
Teshome Geremew https://orcid.org/0000-0002-3858-7105
Tarekegn Tafese https://orcid.org/0009-0001-7785-2987
Milkyas Endale Annisa https://orcid.org/0000-0002-5301-9923

REFERENCES

Angew O.N. (2007). High concentration of vitamin C in orange, Functional foods. *Trends in Food Science and Technology*, *30*, 19-21.

Akinyemi, K.O., Oluwa, O.K., Omomigbehin, E.O., Nuamsetti, T., Dechayuenyong, P., Tantipaibulvut, S., Mohanka, R., Dqg, R., Ri, Q., Wudfwv, P., Materials, A., Pdlqwdlqlqj, D. E., Vdpsohv, W. K. H., Dq, L. Q., Dq, R., Fhqwulixjhg, Z., Usp, D. W., Fhqwulixjh, X., Tfs, E., … Divakar, D. D. (2016). Antibacterial Activity of Citrus sinensis (Orange) Peel on Bacterial Isolates from Wound. *BMC Complementary and Alternative Medicine*, *3*(1), 3374-3381.

Almas, K., Skaug, N., & Ahmad, I. (2005). An in vitro antimicrobial comparison of miswak extract with commercially available non-alcohol mouthrinses. *International Journal of Dental Hygiene*, *3*(1), 18-24.

Ayukekbong, J.A., Ntemgwa, M., & Atabe, A.N. (2017). The threat of antimicrobial resistance in developing countries: Causes and control strategies. *Antimicrobial Resistance and Infection Control*, *6*(1), 1–8.

Azam, S.S., & Abbasi, S.W. (2013). Molecular docking studies for the identification of novel melatoninergic inhibitors for acetylserotonin-O-methyltransferase using different docking routines. *Theoretical Biology and Medical Modelling*, *10*(1), 1-16.

Baba, J., Mohammed, S.B., Ya'aba, Y., & Umaru, F.I. (2018). Antibacterial Activity of Sweet Orange *Citrus sinensis* on some Clinical Bacteria Species Isolated from Wounds. *Journal of Family Medicine and Community Health*, *5*(4), 1154.

Burt S. (2004). Essential oils: their antibacterial properties and potential applications in foods-a review. *International Journal of Food Microbiology*, *94*(3), 223-53.

Bourgou, S., Rahali, F.Z., Ourghemmi, I., Tounsi, M.S. (2012). Changes of peel essential oil composition of four tunisian citrus during fruit maturation. *The Scientific World Journal*, 2012, 1-10.

Crowell, P.L., Gould, M.N. (1994). Chemoprevention and therapy of cancer by d-limonene. *Critical Reviews in Oncogenesis*.5(1), 1-22.

Chee, H.Y., Kim, H., Lee, M.H. (2009). *In vitro* Antifungal Activity of Limonene against Trichophyton rubrum. *Mycobiology*. 37(3), 243-6.

Edogbanya, P.R.O, Suleiman, M.O., Olorunmola, J.B., Oijagbe, (2019). Comparative study on

the antimicrobial effects of essential oils from peels of three citrus fruits. *MOJ Biololgy and Medicine*, *4*(2), 49-54.

Etebu, E., & Nwauzoma, A.B. (2014). A review on sweet orange (*Citrus sinensis*) health, diseases and management. *American Journal of Research Communication*, *2*(2), 33–70.

Friedman, M., Henika, P.R., & Mandrell, R.E. (2002). Bactericidal Activities of Plant Essential Oils and Some of Their Isolated Constituents against *Campylobacter jejuni, Escherichia coli, Listeria monocytogenes,* and *Salmonella enterica*. *Journal of Food Protection*, *65*(10), 1545-1560.

Galma, W., Endale, M., Getaneh, E., Eswaramoorthy, R., Assefa, T., Melaku, Y. (2021). Molecular docking analysis, antibacterial and antioxidant activities of extracts and isolated compounds from the roots extract of *Cucumis prophetarum*, *BMC chemistry*, *15*(32), 1-17.

Hamid, A.A., Aiyelaagbe, O.O., Negi, A.S., Kaneez, F., Luqman, S., Oguntoye, S.O., Kumar, S. B., & Zubair, M. (2019). Isolation and antiproliferative activity of triterpenoids and fatty acids from the leaves and stem of Turraea vogelii Hook. f. ex benth. *Natural Product Research*, *33*(2), 296-301.

Hanuš, L.O., Rosenthal, D., Řezanka, T., Dembitsky, V.M., Moussaief, A.(2008). Fast and easy GC/MS identification of myrrh resins. *Pharmaceutical Chemsitry Journal*, 42(12), 719-20.

Hodek, P., Trefil, P., & Stiborová, M. (2002). Flavonoids-potent and versatile biologically active compounds interacting with cytochromes P450. *Chemico-Biological Interactions*, *139*(1), 1-21.

Koehn, F.E., & Carter, G.T. (2005). The evolving role of natural products in drug discovery. *Nature Reviews Drug Discovery*, *4*(3), 206-220.

Mursiti, S., Lestari, N. A., Febriana, Z., Rosanti, Y.M., Ningsih, T.W. (2019). The activity of Limonene from sweet orange peel (*Citrus sinesis* L.) extract as a natural insecticide controller of bedbugs (*Cimex cimicidae*). *Oriental Journal of Chemistry*, *35*(4), 1420-1425.

Nisha, N.S., Swedha, A.A., Rahaman, J., Basheer J., Sayeed A.(2013). Antibacterial activity of*Citrus sinensis* peel against enteric pathogens. *International Journal of Pharmaceutical Research and Bio-Science*, *2*(5), 1-13.

Nishibe, S., Tamayama, Y., Sasahara, M., & Andary, C. (1995). A phenylethanoid glycoside from Plantago asiatica. *Phytochemistry*, *38*(3), 741-743.

Osarumwense, P.O. (2017). Anti-inflammatory Activity of Methanoilc and Ethanolic Extracts of *Citrus sinensis* peel (L) Osbeck on Carrageenan induced Paw Oedema in Wistar rats. *Journal of Applied Sciences and Environmental Management*, *21*(6), 1223.

Peshin, T., Kar. H.K. (2017). Isolation and Characterization of β-Sitosterol-3-O-βD-glucoside from the Extract of the Flowers of Viola odorata, *British Journal of Pharmaceutical Research*, 16(4), 1-8.

Riffel, A., Medina, L.F., Stefani, V., Santos, R.C., Bizani, D., & Brandelli, A. (2002). *In vitro* antimicrobial activity of a new series of 1,4-naphthoquinones. *Brazilian Journal of Medical and Biological Research*, *35*(7), 811-818.

Safdar, M.N., Kausar, T., Jabbar, S., Mumtaz, A., Ahad, K., & Saddozai, A.A. (2017). Extraction and quantification of polyphenols from kinnow (Citrus reticulate L.) peel using ultrasound and maceration techniques. *Journal of Food and Drug Analysis*, *25*(3), 488-500.

Saini, A., Panesar, P.S., & Bera, M.B. (2019). Comparative Study on the Extraction and Quantification of Polyphenols from Citrus Peels Using Maceration and Ultrasonic Technique. *Current Research in Nutrition and Food Science Journal*, *7*(3), 678-685.

Shetty, S.B., Mahin-Syed-Ismail, P., Varghese, S., Thomas-George, B., Kandathil-Thajuraj, P., Baby, D., Haleem, S., Sreedhar, S., & Devang-Divakar, D. (2016). Antimicrobial effects of *Citrus sinensis* peel extracts against dental caries bacteria: An *in vitro* study. *Journal of Clinical and Experimental Dentistry*, *8*(1), 71-77.

Shimada, T. (2006). Salivary proteins as a defense against dietary tannins. *Journal of Chemical*

Ecology, *32*(6), 1149-1163.

Sofowora, A. (1993). Recent trends in research into African medicinal plants. *Journal of Ethnopharmacology*, *38*(2-3), 197-208.

Sofowora, A. (1996). Research on Medicinal Plants and Traditional Medicine in Africa. *The Journal of Alternative and Complementary Medicine*, *2*(3), 365-372.

Suja, D., Bupesh, G., Nivya, R. Mohan, V., Ramasamy, P., Muthiah, N.S., Arul, A.E., Meenakumari, K., Prabu, K. (2017). Phytochemical Screening, Antioxidant, Antibacterial Activities of Citrus limon and *Citrus Sinensis* Peel Extracts. *International Journal of Pharmacognosy & Chinese Medicine*, *1*(2), 1-7.

Tripoli, E., Guardia, M. La, Giammanco, S., Majo, D. Di, & Giammanco, M. (2007). Citrus flavonoids: Molecular structure, biological activity and nutritional properties: A review. *Food Chemistry*, *104*(2), 466-479.

Uraku, A.J., Uraku, O.H., Nwankwo, V. O.U, Okoye, C.J., Ozioma, P.E., Edenta, C., Ezeali, C., (2020). Medicinal prospective of *Citrus limon* and *Citrus sinensis* peels essential oil by Gas Chromatography/Mass Spectrometry (GC/MS) compositional analysis. *Journal of Bioscience and Biotechnology Discovery*, *5*(3), 53-59.

Williams, C.A., Harborne, J.B., & Clifford, H.T. (1973). Negatively charged flavones and tricin as chemosystematic markers in the palmae. *Phytochemistry*, *12*(10), 2417-2430.

Wong, S.E., & Lightstone, F.C. (2011). Accounting for water molecules in drug design. *Expert Opinion on Drug Discovery*, *6*(1), 65-74.

Young, W.K., Ji, K.M., Young, C.B., Yeon, B.D., Seong, K.L., Seul, M.C., Duck, S.L., Myung, C.C., Kyungsil, Y., Hyung, S.K., (2013). Safety evaluation and risk assessment of d-limonene. *Journal of Toxicology and Enviromental Health Part B.*, *16*, 17-38.